20th Australasian Fluid Mechanics Conference
Perth, Australia
5-8 December 2016

Effect of Medical Imaging Modalities on the simulated blood flow through a 3D reconstructed stented coronary artery segment

C. Scheerlinck[1], C. Mamon[1], T. Zahtila[1], W. Nguyen[1], E. Poon[1], V. Thondapu[1], C. Chin[1], S. Moore[1,2], P. Barlis[1,3] and A. Ooi[1]

[1]Department of Mechanical Engineering
University of Melbourne, Victoria 3010, Australia

[2]IBM Research Australia, Carlton, Victoria 3053, Australia

[3]Department of Medicine, Faculty of Medicine, Dentistry & Health Sciences,
The University of Melbourne, Victoria 3010, Australia

Abstract

Computational fluid dynamics (CFD) studies play an important role in the analysis and prediction of atherosclerosis in coronary arteries. Haemodynamics, in particular endothelial shear stress (ESS), is believed to influence the unhealthy development of the endothelium. In this study, we compared the geometric variances of a patient-specific arterial segment using multiple medical imaging modalities and their effects on haemodynamics. Three-dimensional patient coronary artery reconstructions using standalone X-ray angiography are able to only approximate the artery cross-section as ellipses. On the other hand, intravascular optical coherence tomography (OCT) provides high resolution cross-sectional images of the lumen surface, which can be fused with angiography data to create detailed topographical features of the diseased/scaffold artery segment. The standalone angiography reconstruction is highly automated whereas the OCT-angiography fusion (OCT-A) reconstruction requires manual editing. High fidelity non-Newtonian, pulsatile CFD simulations performed on these 3-D models demonstrate substantial difference in ESS distributions. There is also a higher computational cost associated with performing the OCT-A simulation compared to the angiography simulation.

Introduction

Atherosclerosis is characterized by thickening of the arterial wall due to plaque build-up, and causes stenosis (narrowing) in coronary arteries, which can restrict blood flow. One treatment option is the insertion of a coronary stent (a small mesh tube) into the affected segment of the artery, which expands the narrowed section, allowing increased blood flow. Computational fluid dynamics (CFD) studies have been used to understand the haemodynamic effect of stent placement. It is believed that the haemodynamics inside the artery directly influences the onset and development of atherosclerosis [4, 8]. In particular, low endothelial shear stress (ESS$<$0.4 Pa) has been shown to be a major factor contributing to the build up of plaque [7]. Stenosis typically generates zones of low ESS directly downstream, resulting in further plaque build-up and increased stenosis.

In the past, patient-specific studies have been performed by creating 3-D models of the coronary artery from two standard X-ray angiograms and performing CFD simulations [9]. These models typically approximate the cross-section as an ellipse, with dimensions determined by the width of each 2-D projection from the angiograms [9].

Advanced model reconstruction techniques have been introduced which utilise catheter based imaging techniques such as intravascular ultrasound (IVUS) [11] or intravascular optical coherence tomography (OCT) [8]. OCT pullback produces images with a resolution of 10-20 μm, $\sim$10 times higher than its predecessor, IVUS (100-150 μm) [8]. It uses a fibre-optic cable that can emit light (typically in the infra-red region) and record the back scatter [1]. The laser and camera system is automatically pulled back through the artery at a prefixed speed (20 mm/s) at a specific frame-rate (100 fps), producing a stack of cross-sectional images with a known spacing. More importantly, interior lumen geometries can be exported and fused with the centreline of the lumen from X-ray angiography imaging data to create a highly accurate computer model of a patient-specific coronary artery.

In this study, we reconstructed a segment of a patient-specific artery using both standalone X-ray angiography and OCT-angiography fusion techniques. By considering the identical segment and centreline of the patient's artery, we can perform a side-by-side quantitative comparison of the difference in cross-sectional topographies (such as anatomical changes in lumen cross-section and presence of stent struts, etc.). We also carried out high fidelity CFD studies on each reconstruction. Detailed analysis can elucidate the effects of each reconstruction technique on coronary flow. In particular, this study can lead to better understanding of the influence of medical imaging modalities on the simulated endothelial shear stress (ESS) distribution and thus improve patient outcomes.

Method

Figure 1 shows the steps required to reconstruct a patient-specific artery using standalone X-ray angiography, and OCT-angiography (OCT-A) fusion. A common step in both reconstructions is the detection of lumen centreline using X-ray angiography. Otherwise, standalone angiography approximates the artery cross-section as ellipses along the centreline, whereas OCT-A is able to map real cross-sections onto the centreline.

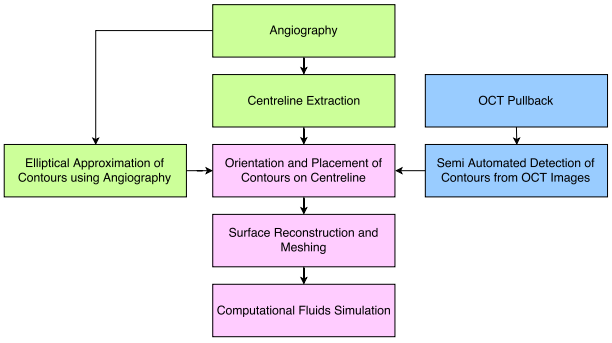

Figure 1: Flowchart outlining patient-specific arterial segment reconstruction methodology.

Angiographic Reconstruction

Angiographic reconstruction uses two individual X-ray angiograms of the artery, at least 35° apart, to calculate the centreline in 3-D space [5]. This is done by creating a surface normal to the plane of the image along the centreline for each image, and solving for the intersection of the two surfaces [2]. The artery cross-section was assumed to be elliptical, and the major and minor axis at each position of the centreline can be calculated using the width of the artery from both angiographic projections. The resulting cross-sectional ellipses were placed normal to the centreline. The aforementioned process was semi-automated using Medis QAngio XA 3D RE 1.1 (Medis Specials BV, Leiden, The Netherlands)

OCT-angiography Fusion Reconstruction

Reconstruction using OCT medical imaging data requires fusion of the artery lumen centreline from X-ray angiography, and corresponding OCT lumen cross-sections. OCT medical imaging data was processed using Medis Qivus 3.0 (Medis Specials BV, Leiden, The Netherlands) and lumen borders were semi-automatically detected and extracted from each image. For embedded struts, both the artery wall and metallic stent struts were combined to form the necessary lumen border, resulting in a closed 2-D contour for each image (figure 2).

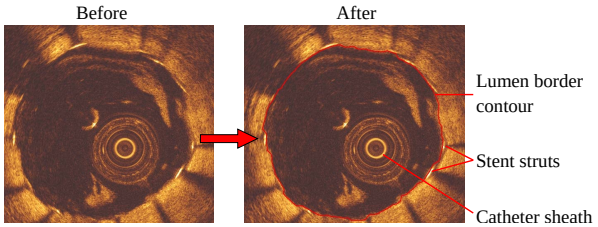

Figure 2: OCT image of lumen border before and after image processing.

The above mentioned OCT lumen contours were placed at an equal longitudinal distance apart (0.2 mm) based on the OCT machine pullback speed and camera frame rate. The OCT contours were mapped onto the identical centreline from the angiography reconstruction. By identifying important anatomical landmarks (such as bifurcations), the proximal and distal locations, and the absolute orientation of the contours on the centreline were determined. A non-uniform rational B-spline surface was constructed using a commercial computer-aided design package (figure 3). It is important to note that despite the catheter path not necessarily coinciding with the centreline, which is indicated by lateral movement of the catheter sheath (figure 2) in OCT images, study has shown that fusion of OCT images with the angiography centreline is a reasonable assumption [3].

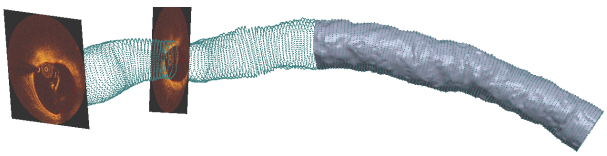

Figure 3: Illustration of OCT-angioagraphy (OCT-A) reconstruction process. From left to right: OCT image contours are mapped to the centreline, then sampled into a cloud of points describing the lumen boundary in (x,y,z) space. A non-uniform rational B-spline surface is generated from this point cloud.

Computational Fluid Dynamics Simulations

The reconstructed patient-specific models from standalone X-ray angiography and OCT-A were discretised into control volumes using ICEM-CFD (ANSYS Inc., Canonsburg, PA, USA). The triangular surfaces were set to be 30 microns in length and the growth rate of tetrahedral elements away from the arterial wall was set to 1.1. The total amount of tetrahedral elements were ∼20 and ∼25 million for standalone angiography and OCT-A reconstructions, respectively.

High fidelity CFD simulations were performed using OpenFOAM 2.1.1 (OpenCFD Ltd, ESI group, Bracknell, UK) that directly solved the incompressible Navier-Stokes equations. Human blood exhibits shear thinning behaviour as a result of red blood cell deformation and this behaviour was accounted for by employing the Quemada model [10]. To mimic the cyclic variation of flow through a coronary artery, a pulsatile inlet velocity waveform was used [12], which is consistent with in vivo physiological conditions (i.e. human heartbeat), and was chosen to maintain an equivalent flow rate for each model. The cycle period (cardiac cycle) is 0.8 seconds, and the simulation is carried out for three cycles in order to ensure that all transients have been convected out of the computational domain. Only the data of the final cycle is used for analysis. The following boundary conditions were applied:

1. Pulsatile uniform velocity at the inlet (figure 4)
2. No-slip at the artery wall and stent struts
3. Zero pressure at the outlet

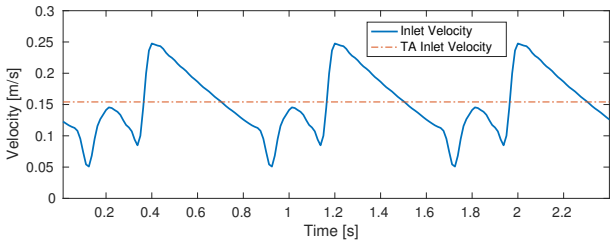

Figure 4: Pulsatile inlet velocity waveform and time-averaged inlet velocity for OCT-A case.

Results

Reconstruction

The standalone angiography reconstruction technique is unable to fully capture detailed 3-D surface features, since only two 2-D projections are used. Hence the cross-section is approximated as a sequence of ellipses, which results in a non-physiological, smooth surface (figure 5). In contrast, the OCT-A reconstruction has an uneven surface as OCT medical imaging data can accurately capture lumen contours as well as the strut locations in the artery, which cannot be detected using X-ray angiography.

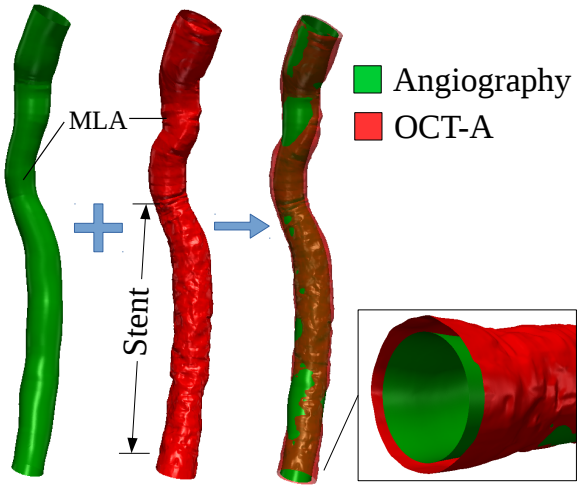

Figure 5: Angiography and OCT-A surfaces superimposed for comparison, with cutaway showing cross section, and minimal lumen area (MLA) and stent locations indicated.

Figure 6 shows a large variation in cross-sectional area of the OCT-A reconstruction compared to the angiography reconstruction along the considered segment. This is due to the approximation of irregular cross-sectional lumen geometries as ellipses by the angiography reconstruction. OCT-A shows a larger inlet cross-sectional area (approximately 1.12 times larger) than the angiography case. As a result, the inlet velocity for the OCT-A is lower than the angiography case for a given flow rate (0.137 m/s versus 0.154 m/s).

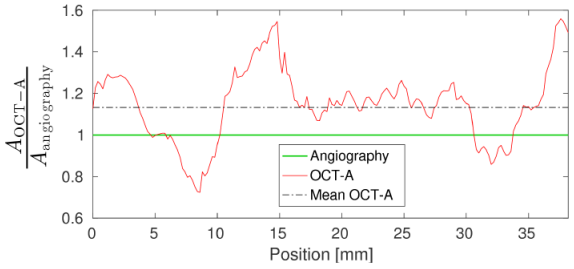

Figure 6: Relative cross-sectional area (A) of OCT-A to angiography reconstruction along the centerline, with the proximal end at Position = 0 mm.

A summary of the important quantitative geometric parameters can be found in table 1. The position of the minimal lumen area (MLA) of the OCT-A is 4.2 mm closer to the proximal end compared to the MLA location of the angiography. The tendancy of the angiography reconstruction to underestimate the cross-sectional area is reflected in the difference in volume between the OCT-A and angiography (46.2 mm^3).

Parameter	Angiography	OCT-A	Difference
Minimal lumen area (MLA)	4.70 mm^2	5.33 mm^2	0.63 mm^2
Stenosis location*	13 mm	8.8 mm	4.2 mm
Total surface area	338.2 mm^2	381.4 mm^2	43.2 mm^2
Total volume	240.4 mm^3	286.6 mm^3	46.2 mm^3

**distance from proximal end*

Table 1: Comparison of key geometric parameters.

CFD Simulation

Time-averaged endothelial shear stress (TA-ESS) is calculated by averaging the endothelial shear stress over the third cardiac cycle. Results of both angiography and OCT-A are presented in figure 7.

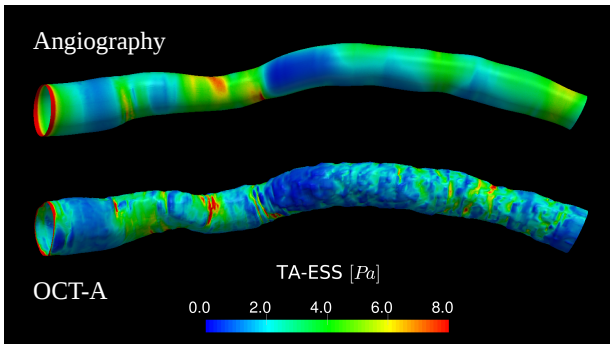

Figure 7: TA-ESS distribution for angiography and OCT-A reconstruction. The high TA-ESS on the left (inlet) is an artefact of computational noise.

Figure 8 shows a histogram of the percentage surface area of non-dimensionalised TA-ESS. In order to account for the different inlet velocities (due to the variation in inlet cross-sectional area), TA-ESS is non-dimensionalised by dividing by $0.5\rho\bar{U}^2$, where $\bar{U}$ is the average inlet velocity over one cycle, and $\rho = 1060$ kg/m^3. Bin intervals for the non-dimensionalised TA-ESS are set at 0.05 units. This corresponds to a bin interval of 0.5 Pa in TA-ESS. In brief, the first histogram bar lies within 0-0.05 non-dimensionalised TA-ESS (or in other words within the atherogenic ESS regime of 0-0.5 Pa). This bar therefore indicates the percentage of lumen surface area with a high risk of adverse clinical outcomes such as plaque development. OCT-A results in a larger percentage area with non-dimensionalised TA-ESS in this first interval compared to angiography, which highlights the potential benefit of using OCT-A in a clinical setting.

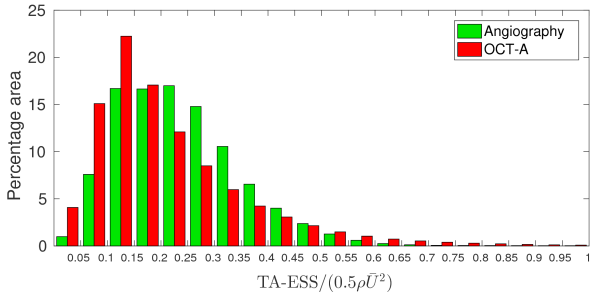

Figure 8: Histogram of the percentage surface area versus non-dimensionalised TA-ESS.

Discussion

OCT medical imaging data, when fused with the centreline from X-ray angiography to reconstruct a three dimensional patient-specific scaffold artery segment, is able to provide unprecedented detail of the lumen cross-section and stent strut placement. In addition, standalone angiograhy reconstruction and OCT-A result in different minimal lumen area (MLA) and stenosis location.

Geometric variation between the angiography and OCT-A reconstructions result in different simulated flow fields. Low ESS

regions typically occur distal to stenosis due to recirculation, and is consistent with our results (figure 7). The variation in cross-sectional area along the artery segment of OCT-A compared to angiography reconstructions ($\sim$20-50%) impacts the flow field by virtue of conservation of mass (i.e. narrower regions accelerate the flow) and the resultant increase in velocity tends to increase ESS and vice versa. This means that error in cross-sectional area can lead to inaccurate ESS distributions from simulations. The ability of OCT to capture individual stent struts is a major advantage compared to angiography because stent struts have a significant impact on the flow, causing higher ESS on the strut surface, and lower ESS in their wake [6]. The smooth surface of the angiography reconstruction leads to a more uniform TA-ESS distribution, in contrast with the OCT-A case, which resulted in localised pockets of high and low TA-ESS. This occurs around the natural wrinkles of the arterial wall and the stent struts (figure 7). The OCT-A case results in more percentage surface area with high, and low TA-ESS (figure 8), and has $\sim$4% surface area with critically low TA-ESS ($<$0.05 units of non-dimensionalised TA-ESS), which is $\sim$3 times more than the angiography case.

Performing in vivo intravascular OCT pullback as well as X-ray angiography is more expensive and time-consuming than angiography alone. In our study, the total execution time of the OCT-A simulation was 9 days, and the angiography was 7 days and 14 hours, indicating a higher computational cost associated with the OCT-A case. OCT-A reconstruction also takes more time because manual editing is required to correct errors in automatic lumen detection. Future direction could include the development of more robust automation of the OCT-A reconstruction.

Conclusions

Our studies show that coronary artery reconstruction from fusion of OCT-angiography medical imaging data provides an ESS distribution that captures the effect of stents and irregular artery cross-sections on coronary haemodynamics. Standalone angiography is limited to produce smooth, elliptical models which are not physiological. Comparison of CFD studies between standalone angiography and OCT-A reconstructions of the same artery resulted in different TA-ESS distributions. Importantly, the OCT-A case yielded higher percentage surface area of low TA-ESS. This highlights the potential application of OCT derived CFD studies and the role for such models in helping to guide intervention procedures and improve outcomes into the future.

Acknowledgements

This research was supported by a Victorian Life Sciences Computation Initiative (VLSCI) grant number [VR0210] on its Peak Computing Facility at the University of Melbourne, an initiative of the Victorian Government, Australia.

References

[1] Bezerra, H. G., Costa, M. A., Guagliumi, G., Rollins, A. M. and Simon, D. I., Intracoronary optical coherence tomography: a comprehensive review clinical and research applications, *JACC Cardiovasc Interv*, **2**, 2009, 1035–46.

[2] Bourantas, C. V., Kourtis, I. C., Plissiti, M. E., Fotiadis, D. I., Katsouras, C. S., Papafaklis, M. I. and Michalis, L. K., A method for 3d reconstruction of coronary arteries using biplane angiography and intravascular ultrasound images, *Comput Med Imaging Graph*, **29**, 2005, 597–606.

[3] Bourantas, C. V., Papafaklis, M. I., Athanasiou, L., Kalatzis, F. G., Naka, K. K., Siogkas, P. K., Takahashi, S., Saito, S., Fotiadis, D. I., Feldman, C. L., Stone, P. H. and Michalis, L. K., A new methodology for accurate 3-dimensional coronary artery reconstruction using routine intravascular ultrasound and angiographic data: implications for widespread assessment of endothelial shear stress in humans, *EuroIntervention*, **9**, 2013, 582–93.

[4] Gijsen, F., van der Giessen, A., van der Steen, A. and Wentzel, J., Shear stress and advanced atherosclerosis in human coronary arteries, *J Biomech*, **46**, 2013, 240–7.

[5] Gijsen, F. J., Wentzel, J. J., Thury, A., Lamers, B., Schuurbiers, J. C., Serruys, P. W. and van der Steen, A. F., A new imaging technique to study 3-d plaque and shear stress distribution in human coronary artery bifurcations in vivo, *J Biomech*, **40**, 2007, 2349–57.

[6] LaDisa, J. F., J., Guler, I., Olson, L. E., Hettrick, D. A., Kersten, J. R., Warltier, D. C. and Pagel, P. S., Three-dimensional computational fluid dynamics modeling of alterations in coronary wall shear stress produced by stent implantation, *Ann Biomed Eng*, **31**, 2003, 972–80.

[7] Malek, A. M., Alper, S. L. and Izumo, S., Hemodynamic shear stress and its role in atherosclerosis, *JAMA*, **282**, 1999, 2035–42.

[8] Papafaklis, M. I., Bourantas, C. V., Yonetsu, T., Vergallo, R., Kotsia, A., Nakatani, S., Lakkas, L. S., Athanasiou, L. S., Naka, K. K., Fotiadis, D. I., Feldman, C. L., Stone, P. H., Serruys, P. W., Jang, I. K. and Michalis, L. K., Anatomically correct three-dimensional coronary artery reconstruction using frequency domain optical coherence tomographic and angiographic data: head-to-head comparison with intravascular ultrasound for endothelial shear stress assessment in humans, *EuroIntervention*, **11**, 2015, 407–15.

[9] Poon, E. K., Hayat, U., Thondapu, V., Ooi, A. S., Ul Haq, M. A., Moore, S., Foin, N., Tu, S., Chin, C., Monty, J. P., Marusic, I. and Barlis, P., Advances in three-dimensional coronary imaging and computational fluid dynamics: is virtual fractional flow reserve more than just a pretty picture?, *Coron Artery Dis*, **26 Suppl 1**, 2015, e43–54.

[10] Popel, A. S. and Enden, G., An analytical solution for steady flow of a quemada fluid in a circular tube, *Rheologica Acta*, **32**, 1993, 5.

[11] Prause, G. P., DeJong, S. C., McKay, C. R. and Sonka, M., Towards a geometrically correct 3-d reconstruction of tortuous coronary arteries based on biplane angiography and intravascular ultrasound, *Int J Card Imaging*, **13**, 1997, 451–62.

[12] Womersley, J. R., Method for the calculation of velocity, rate of flow and viscous drag in arteries when the pressure gradient is known, *J Physiol*, **127**, 1955, 553–63.